Alpha-synuclein phosphorylation is abundant in the non-synucleinopathy human brain

[1]Choi S., [1]Duvernay J., [1]Bahrami A., [1]Tittle T., [2]Sani S., [3]Kordower JH, [3]Muller S., [1]Killinger BA

[1]Department of Neurological Sciences, Rush University Medical Center, Chicago, IL, USA

[2]Department of Neurological Surgery, Rush University Medical Center, Chicago, IL, USA.

[3]ASU-Banner Neurodegenerative Disease Research Center and School of Life Sciences, Arizona State University, Tempe, AZ, USA

Abstract

Phosphorylation of alpha-synuclein at serine 129 (PS129) has been strongly associated with aggregates and implicated in the synucleinopathy disease processes. Recent findings suggest that PS129 is abundant in the non-synucleinopathy mammalian brain, in a brain region-specific and context-dependent manner, raising important questions about the significance of PS129 for synucleinopathy disease processes. Here, we identified and described phosphatase labile physiological PS129 in the mammalian brain using a range of specimens from rodent to human surgically resected temporal lobectomy tissues. Results confirmed phosphatase-sensitive physiological PS129 in the non-synucleinopathy human temporal lobe and hippocampus when the post-mortem interval was eliminated (i.e., surgically resected human samples or perfusion-fixed animal brain). In the non-synucleinopathy mammalian brain, PS129 fluctuated between 2-45% of the total asyn pool in a case-specific and brain region-specific manner. In agreement with previous studies, physiological PS129 was abundantly distributed throughout the layers of the hippocampus and cortex. Physiological PS129 was not observed in PD brain, or non-synucleinopathy specimens of >2h post-mortem interval. Remarkably, in the PD brain, the PS129 to asyn ratio was similar (~5-40%) to that in the non-synucleinopathy brain. Despite physiological PS129 being associated with neuronal activity, physiological PS129 did not correlate with cFos expression. Conclusions: Physiological PS129 is abundant in the human brain, and

apparent pathological enrichment, in part, can be explained by the enzymatic resistance of aggregates and not disease-driven phosphorylation events.

Introduction

Alpha-synuclein is a protein that misfolds and accumulates in the brain of diseases collectively referred to as synucleinopathies. Alpha-synuclein can be phosphorylated at serine 129 (PS129)[1]. PS129 in the postmortem brain has served as a reliable marker of pathogenic alpha-synuclein aggregates[2], because in the diseased brain, an estimated 90% of aggregated alpha-synuclein is PS129, while physiological PS129 has been estimated to be approximately 4% or less[2] (although these estimates may vary widely based on context and brain region[3]). Despite the potential importance for understanding disease, it's unclear if PS129 plays a protective, toxic, or neutral role[4-9].

Recent discoveries have demonstrated that alpha-synuclein phosphorylation occurs in the healthy mammalian brain, results from neuronal activation, and PS129 may play a role in signaling protein-protein interactions[3, 10, 11], but understanding physiological PS129 in the context of the non-diseased brain has been challenging[12]. A technical challenge has been highlighted by several studies that suggested that physiological PS129 is rapidly dephosphorylated following death[2, 13], making post-mortem PS129 measurements unreliable. Theoretically, brain tissues lacking a post-mortem interval would be required to measure physiological-PS129. One such possibility are tissues from temporal lobectomies, which are performed on rare intractable cases of epilepsy where a small portion of the temporal lobe and

hippocampus/amygdala are surgically resected. In the mammalian brain, PS129 is found most abundantly in the olfactory bulb and hippocampus, making temporal lobectomy resected tissues optimal for establishing human PS129.

Here we present results from experiments characterizing physiological PS129 in an array of specimens, including rapidly preserved surgically resected human brain specimens.

Materials and Methods

Tissues

All procedures were approved by the Institutional Review Board at Rush University Medical Center. Free-floating PD/DLB hippocampal samples were obtained from the Rush Movement Disorders Brain Bank. FFPE hippocampal sections from control and PD cases with short postmortem intervals (2-3 hours) were obtained from the Brain and Body Donation Program at Banner Sun Health Research Institute. Details regarding all human specimens used in these studies are shown in Table 1.

All animal procedures were reviewed and approved by the Rush University Medical Center Institutional Animal Care and Use Committee. Non-treated cynomolgus monkeys ranging from 4 to 15 years of age and C57BL/6J male and female mice (RRID: IMSR_JAX:000664) from 4–8 months of age were used in animal studies. Animal specimen characteristics are detailed in Table 2.

Tissue fixation

Upon tissue resection from epileptic patients, samples were immediately placed in 4% paraformaldehyde (PFA) solution in 0.1 M phosphate-buffered saline (PBS, pH 7.4) or first rinsed in PBS for a few minutes and then transferred to 4% PFA. All tissues

underwent fixation for at least 72 hours, followed by equilibration in 15% and then 30% sucrose solutions. Tissues were then coronally sectioned at 40 μm thickness using a freezing stage sliding knife microtome (American Optical) (RRID:SCR_018434). The sections were stored in a cryoprotectant solution (30% sucrose, 30% ethylene glycol in PBS) at −20 °C until further processing.

Immunohistochemistry

Free-floating tissues were washed in dilution media (DM, 50 mM Tris–HCl pH 7.4, 150 mM NaCl, 0.5% Triton-X100) three times, 10 minutes each, followed by heat-induced antigen retrieval (HIAR) for 30 minutes in sodium citrate buffer (10 mM Sodium Citrate, 0.05% Tween 20, pH 6.0) at 90°C. The solution was cooled down to room temperature, and the tissues were rinsed in DM once. Sections were incubated in peroxidase quenching solution (0.3% hydrogen peroxide, 0.1% sodium azide) containing blocking buffer (3% goat serum, 2% BSA, 0.4% Triton X-100 in DM) for 1 hour at room temperature. Sections were briefly washed in DM and incubated with PS129 antibody (Abcam, EP1536Y, RRID:AB_765074) or c-Fos antibody (Abcam, Cat#: ab190289, RRID:AB_2737414) at a dilution of 1:50,000 or 1:10,000, respectively, in blocking buffer overnight at 4°C. The next day, tissues were rinsed in DM three times, 10 minutes each. Sections were incubated with HRP-conjugated goat anti-rabbit secondary antibody (Thermo Fisher Scientific, Cat#: 31462, RRID:AB_228338) at a dilution of 1:1,000 in DM containing 1% BSA, 1% goat serum for 1 hour at room temperature. Samples were rinsed in DM 2 times, and once in sodium acetate buffer (0.2 M Imidazole, 1.0 M sodium acetate buffer, pH 7.2), 10 minutes each, and developed using a standard nickel-enhanced 3,3′-diaminobenzidine (DAB)-imidazole

protocol. Sections were rinsed with sodium acetate buffer and PBS, and mounted on charged slides (Superfrost Plus Microscope Slides, Fisher, Cat#: 22-034-979) or gelatin-coated glass slides, completely dried, counterstained with purified methyl green (Sigma-Aldrich, Cat#67060), dehydrated, cleaned with xylenes (Fisher, Cat# X3P-1GAL), and cover-slipped with Cytosol XYL (Epredia, Ref#: 8312-4).

In situ enzymatic pretreatment

Before immunoassay, matching tissues were subjected to treatment with or without calf-intestinal alkaline phosphatase (CIAP) or proteinase K (PK). For the CIAP treatment, tissues were incubated with CIAP enzyme (Promega, Cat#: M2825, 20u/µL) at a 1:333 dilution in CIAP buffer (100 mM NaCl, 10 mM $MgCl_2$, and 50 mM Tris–HCl at pH 7.9) for 24 hours at 37°C prior to subsequent assays, following previously established protocols [14]. For PK treatment, tissues were incubated with the PK (Thermo Sceintific, Cat#: EO0491, ~20mg/mL) diluted 1:1,000 in PBS at 37°C for 10 minutes before proceeding with the remaining assay steps [14].

Protein extraction

Proteins were extracted from fixed floating tissue sections as described previously[13] (see protocols.io https://dx.doi.org/10.17504/protocols.io.36wgq3xyylk5/v1). Then 100 µL of solubilized samples in crosslink reversal buffer (5% SDS, 0.5 M EDTA pH8.0, 0.5 M Tris-Base, 0.150 M NaCl) were mixed with 400 µL methanol (Sigma Aldrich, Cat#: 179337), 100 µL chloroform (Sigma Aldrich, Cat#: C2432), and 300 µL ultrapure water. Following each addition, samples were vigorously vortexed for approximately 10 seconds. The mixtures were then centrifuged at 14,000g for 2 minutes, and the top aqueous layer was

removed. Subsequently, 400 μL of methanol was added to each sample, vortexed, and centrifuged at 14,000g for 3 minutes. After removing the methanol, the pellets were air-dried for approximately 10 minutes before resuspension in 5% SDS solution. These samples were then processed for further assays.

Spot blotting

1 μl of each protein sample was spotted onto a methanol-activated PVDF membrane, followed by complete drying. The membrane was reactivated with methanol and washed in ultrapure water, followed by post-fixation in 4% PFA for 30 minutes. The blots were subsequently rinsed in water again, and probed for total protein stain, followed by rinsing in water and TBST (20 mM Tris–HCl pH 7.6, 150 mM NaCl, 0.1% Tween-20), then immersion in blocking buffer (5% dry milk in TBST) for 1 h at room temperature. The membrane was incubated overnight at 4°C with the anti-αsyn antibody (BD Biosciences, #610787, RRID:AB_398108 or Abcam, EPR20535, RRID:AB_2941889) diluted 1:2,000 or 1:20,000, respectively, in blocking buffer. The next day, blots were washed and incubated with secondary antibodies (anti-mouse HRP conjugate at 1:6,000, RRID:AB_330924, and anti-rabbit HRP conjugate at 1:20,000) diluted in blocking buffer. Following another round of washing with TBST, blots were imaged using chemiluminescence substrates with a Chemidoc Imager (RRID:SCR_019037).

Western blotting

10 μg of proteins were separated using 4–12% Bis–Tris gels (Invitrogen, Ref#: NW04125BOX) with MES SDS Running Buffer (Invitrogen, Ref#: B002), and blotted onto methanol-activated polyvinylidene difluoride (PVDF) membrane (Immobilon-FL

Membrane, Merck Millipore Ltd, Cat#: IPFL00010). The membrane was dried completely and reactivated using methanol followed by fixation in 4% PFA for 30 min, rinsed in ultrapure water two times, and stained for total protein (Licor, Revert 700 Total Protein Stain Kit, Part#: 926-11010). Upon imaging the total protein with Odyssey M imager (Li-Cor) (RRID:SCR_025709), blots were destained using Revert 700 destaining solution, followed by rinsing in TBST and placed in blocking buffer (5% dry milk in TBST) for 1 h at room temperature. Blots were incubated overnight at 4°C with PS129 diluted 1:50,000 or SYN1 (BD Biosciences Cat# 610787) diluted 1:2,000 in blocking buffer. The following day, blots were washed in TBST three times, 10 minutes each, and incubated with goat anti-rabbit HRP conjugate at 1:20,000, or horse anti-mouse HRP conjugate (Cell Signaling Technology Cat# 7076, RRID:AB_330924) at 1:6,000 dilution in the blocking buffer for 1 h at room temperature. Membranes were washed again in TBST three times and imaged using chemiluminescence substrates (Clarity Western ECL Substrate, Bio-Rad, product # 170–5060 or Super Signal West Atto Ultimate Sensitivity Chemiluminescence Substrate, Thermo Scientific, Ref#: A38554) with a Chemidoc imager (Bio-Rad) (RRID:SCR_019037). For quantification of band intensities, the optimal auto-exposure setting was applied during imaging, and the resulting raw TIFF files were analyzed using ImageJ (version 1.54g, RRID:SCR_003070).

Measurement of PS129: aSyn ratio

1 µl of solubilized sample was spotted onto two membranes simultaneously, and each was probed for aSyn or PS129. From solubilization of samples to imaging, samples from the same species (i.e., human, monkey, or mouse) were processed together for all steps. For imaging, the blots were exposed to chemiluminescence

substrate for 5 minutes and imaged simultaneously using a Chemidoc imager with optimal auto-exposure settings. This setting generates quantitative images by determining the exposure time, ensuring that bright bands are saturated while faint bands remain detectable. The raw TIFF image file was then opened in ImageJ, and the signal intensities were measured for aSyn and PS129 at the same time. The areas measured for PS129 and aSyn were exported and compared for the ratio. The results were then graphed, and a Two-way ANOVA with Tukey post-hoc testing was conducted using GraphPad Prism 10.

Results

Physiological PS129 was exclusively detected in surgical specimens

Physiological PS129 occurs in the healthy mammalian brain but has not been unambiguously identified in the non-synucleinopathy human brain, potentially due to artifactual post-mortem dephosphorylation [2, 14]. To establish the basal existence of PS129 in the human brain, we characterized PS129 within surgically resected brain tissues from temporal lobectomy procedures. Depending on the patient's condition, the resection included portions of the inferior and medial temporal gyri covering the hippocampus, the hippocampus, and the amygdala anterior to the hippocampus. Following resection by neurosurgeons, tissues were either immediately fixed in 4% PFA or briefly immersed in saline before fixation.

Immunohistochemical analysis revealed PS129 positivity in both the resected hippocampus (Fig. 1A) and temporal cortex (Fig. 1B), with signals predominantly localized throughout the gray matter. Within specific gray matter regions, intensely labeled PS129-positive perikarya were observed, with several neurons displaying

distinct PS129-positive projections. Notably, diffuse punctate structures of PS129 reactivity were consistently detected across all PS129-positive regions, with some regions showing more apparent labeling than others, similar to previous reports [3, 14]. To validate the specificity of PS129 reactivity, we performed in situ enzymatic pre-treatments with either CIAP or PK. These treatments were selected based on our recent findings that αSyn aggregates demonstrate CIAP resistance, while limited PK digestion has been widely established as a method to increase immunolabeling specificity for aggregates [14-16]. We tested whether the PS129 identified in these surgical samples displays resistance to CIAP and/or PK treatment. The result showed that PS129 immunoreactivity was completely abolished by both enzymes, indicating that the detected signals represent the presence of non-aggregated biological PS129 in the non-synucleinopathy human brains.

PS129 immunoreactivity patterns in surgical samples were then compared with those in post-mortem PD/DLB brain tissues, which were obtained from autopsies with post-mortem intervals exceeding 6 hours before fixation. Hemisections were used to mitigate any possible regional differences when comparing the variably sampled surgical with postmortem brains. PS129 staining of PD brain hemisection (Fig. 1C) revealed widespread PS129 distribution throughout the gray matter, including the hippocampus (red box) and mid-inferior temporal cortex (blue box) adjacent to the hippocampal formation, making it difficult to distinguish pathological brain tissue from surgical samples based on abundance and distribution alone. However, detailed examination at higher magnification revealed distinct morphological differences; the hippocampus and mid-inferior temporal cortex exhibited clear, dense Lewy bodies and

Lewy neurites [17], in contrast to the diffuse punctate pattern observed in surgical samples. Importantly, PD hemisections pretreated with CIAP retained PS129 staining despite slightly reduced overall signal, confirming that these PS129-positive signals represent aggregated, pathological forms of α-synuclein.

After characterizing PS129 distribution and qualitative morphology in surgical samples and PD/DLB hippocampal sections (Fig. 1 and Fig. S1), we conducted western blot analyses with CIAP or PK pre-treatments to quantify the influence of enzymatic pretreatment on PS129. PS129 immunoblotting results agreed with our immunohistochemical staining, showing almost complete elimination of PS129 signals in surgical samples following CIAP or PK treatment (Two-way ANOVA, $F(1.405, 9.837) = 17.68$, $P = 0.0010$, and $F(7, 14) = 6.656$, $P = 0.0014$, respectively, for surgical temporal cortex samples) whereas one PD hippocampus sample exhibited only partial reduction of PS129 signal (Fig 2A and B). Interestingly, in two other PD/DLB hippocampus tissues (Fig. 2B), PS129 levels in negative controls (no-enzyme pretreatment) were substantially lower compared to those of surgical samples loaded on the same gels. Notably, PK pre-treatment enhanced signal detection in these samples—a finding that is consistent with our immunohistochemical staining results (SF1). The observed variability in PS129 solubility across the three PD/DLB hippocampal samples likely reflects the inherent clinical and pathological heterogeneity of synucleinopathies [18-20]. Furthermore, higher PS129 signals in the two PD/DLB cases after PK treatment can be explained by previous reports showing that PK pretreatment enhances the immunoreactivity of abnormal α-synuclein, especially in the hippocampus and temporal cortex [18, 21]. Total αSyn levels (Fig. 2C) remained unchanged following CIAP

treatment in both surgical and PD/DLB cases. Although PK digestion enhanced PS129 reactivity, total αSyn was not detected by the commonly used total αSyn antibody (BD SYN1, RRID: AB_398107) [22]. This antibodies epitope (amino acids 91-99) may be cleaved by PK, or potentially the NAC domain-overlapping epitope is “hidden” within aggregates [15, 16].

Quantification of the PS129 and aSyn signals in 7 surgical samples and 3 PD/DLB hippocampal specimens (Fig. 2B-C) confirmed that αSyn observed in the surgical samples exists in non-aggregated forms, as evidenced by its sensitivity to enzymatic treatments. In contrast, αSyn in PD/DLB samples consists of enzymatically resistant aggregates, with PK treatment enhancing PS129 detection in some cases rather than abolishing it.

Physiological PS129 is more abundant than previously estimated

Current literature estimates physiological PS129 levels in the normal rat brain at approximately 4% of total αSyn [2]. This phosphorylated form undergoes rapid dephosphorylation after death, with levels declining significantly by 30 minutes post-mortem and becoming undetectable within one hour [2, 14]. We investigated whether human brains also have physiological PS129, and if they do, how much PS129 exists in the total pool of aSyn. Using spot blotting techniques on surgical tissues, we probed the samples for PS129 and total αSyn, and quantified signals to establish relative abundance ratios between PS129 and αSyn within each specimen.

Surgical samples exhibited a wide range of PS129 to αSyn ratios (Fig. 3A and B), ranging from approximately 10% to over 40%. This observation is remarkable, as these values substantially exceed what has been previously reported. Recent studies have

demonstrated that neuronal activity increases PS129 levels [10, 11]. To investigate whether the elevated PS129 levels stem from increased neuronal activity, we examined whether these tissues exhibit c-Fos activation that correlates with the high PS129 levels. c-Fos is an indicator of neuronal activity and also exhibits the strongest correlation between gene expression and epileptiform activity [23-25], especially in the temporal cortex and hippocampus [23, 24, 26]. c-Fos immunohistochemistry revealed that all surgical samples contained c-Fos-positive cells, although reactivity was moderate across all specimens. Within individual cases, varying intensities of immunoreactivity were observed throughout different regions. Notably, the density of c-Fos-positive cells did not appear to correlate with PS129 levels detected in the same samples. These findings suggest that while neuronal activity may influence PS129 accumulation, PS129 detection appears to be affected by additional factors, such as the time interval between tissue resection and fixation. The two cases with the highest PS129: αSyn ratios (TC1 and HIP1) were immediately fixed in 4% PFA upon resection. In contrast, TC3, TC4, and HIP2 samples were initially placed in saline and transferred to 4% PFA within minutes. The TC5 sample experienced a more substantial delay (approximately 10-15 minutes) before PFA fixation. Table 1 provides comprehensive clinical and procedural information for each case.

The PS129 to aSyn ratio in PD/DLB hippocampus tissues (Fig. 3C and D) exhibited variability consistent with western blot findings (Fig. 2). For example, in the HIP3 (PD), harsh crosslink reversal buffer (containing 5% SDS with 30-minute boiling) solubilized less than 20% of PS129, while two additional cases showed PS129 levels below the detection threshold of optimal auto-exposure settings. PK treatment

enhanced PS129 detection in all cases. Since the BD SYN1 antibody failed to detect aSyn in PK-treated samples, we employed an alternative antibody (EPR20535) for total aSyn detection and subsequent quantification. Despite this antibody substitution resulted in lower detected aSyn levels compared to untreated samples. Across PD hippocampus samples (HIP1-3), the solubilized PS129 to aSyn ratio remained below 20%. Further analysis of residual pellets from the HIP3 sample, when solubilized in urea buffer [2], demonstrated that some PS129 remained unextracted. In contrast, surgical samples exhibited the absence of PS129 in their corresponding pellet fractions (SF2), indicating that extraction efficacy of asyn/PS129 was much higher in surgical samples, and the ratio measured in surgical samples using the solubilized supernatant accurately reflects the abundance of PS129 relative to aSyn ratio in the whole tissue.

Physiological PS129 in the brain of other mammals

To examine whether measured PS129 in human brains was conserved across other mammalian brains, monkey and mouse hippocampus and temporal cortex tissues were assessed for PS129 to aSyn ratio. Mouse brains have been well-documented for having abundant PS129 levels, especially in the olfactory bulb and in the hippocampus [3, 11]; however, the amount of PS129 to αSyn was yet to be determined. Further, monkey brain has never been assessed for physiological PS129 other than in the olfactory bulb in our previous report [3].

We first assessed whether monkey brain tissues have physiological PS129. Strikingly, PS129 immunostaining on coronal sections of *Macaca fascicularis* (commonly known as cynomolgus macaque) revealed abundant physiological PS129 throughout the brain, especially in gray matter (Fig. 4A). This pattern resembled what was observed

in the human brain (Fig. 1). Under higher magnification of hippocampus (red box) and middle temporal gyrus (blue box), perikarya with dense physiological PS129 were observed along with diffuse punctate structures throughout the gray matter, similar to patterns seen in Fig. 1 (Fig. 4A).

Hippocampus and middle temporal gyrus (referenced from the Scalable Brain Atlas[27]) were isolated from five monkeys and probed for PS129 and αSyn using the same methodology as for human samples. Results showed that most cases (Monkeys 2-5) had ratios of approximately 2-5%, with the hippocampus displaying slightly higher PS129 abundance than the temporal cortex. Notably, Monkey 1 exhibited substantially higher PS129 levels, about 19% and 25% for the hippocampus and temporal cortex, respectively. For mouse brain samples, specifically hippocampus and isocortex surrounding the hippocampal formation, PS129 to αSyn ratios exhibited greater variation, ranging from approximately 3-10% across both regions. Interestingly, four of the five mice, the temporal cortex displayed slightly elevated PS129 levels compared to the hippocampus.

c-Fos activity across all animals assessed was variable and did not correlate with PS129 abundance (SF3). Monkey 1, despite having the highest PS129 levels, showed rare c-Fos activation in hippocampal tissue, with signal levels similar to other monkey brains that exhibited substantially lower PS129 levels. For mice, cortical areas showed abundant c-Fos activation with some c-Fos-positive cells in the hippocampus, similar to other reports [28, 29].

Rapid post-mortem dephosphorylation of physiological PS129 in human brains

To investigate whether physiological PS129 could be preserved in human autopsy specimens, we analyzed formalin-fixed hippocampal tissues obtained within markedly short post-mortem intervals (2-3 hours) (detailed PMIs documented in Table 1). These specimens underwent immunostaining for PS129 with and without CIAP pretreatment to differentiate physiological from aggregated PS129, respectively. Our findings revealed that even with post-mortem intervals as brief as two hours, physiological PS129 signals were not detectable in human brain tissues (Fig. 5 and SF4). Control/non-synucleinopathy specimens lacked PS129 immunoreactivity with or without CIAP, while PD hippocampal samples had apparent Lewy bodies and neurites with and without CIAP treatment. Critically, the characteristic physiological PS129 labeling pattern (e.g., diffuse punctate pattern throughout grey matter and the layers of the hippocampus) was consistently absent across all examined specimens, suggesting post-mortem dephosphorylation of physiological PS129 within 2h, consistent with previous findings in mouse brain[13].

Discussion

Here, we add further evidence that PS129 is a common form of aSyn within the human brain. This differs from the contemporary understanding that PS129 is a disease-specific modification. Instead, this work, along with other findings, strongly suggests PS129 is not an inherently disease-associated modification but likely “enriched" in aSyn due to conformational restrictions to enzymatic liability. Following death, intracellular ATP levels rapidly decrease, restricting post-mortem kinase activity but allowing continued post-mortem phosphatase activity[30, 31]. In the context of post-mortem specimens, only P129 within aggregates cannot be dephosphorylated, and thus

preserved[13], accounting for the phenomenon of PS129 enrichment. This hypothesis requires that PS129 is detectable in brain specimens lacking a post-mortem interval, which we established here in rapidly preserved surgically resected temporal lobectomy specimens. Remarkably, we measured PS129:asyn upwards of 43% in the non-synucleinopathy brain, well above previous estimates. PS129 from non-synucleinopathy brain was distinguishable from PD brain by enzymatic properties (i.e., phosphatase, protease resistance), tissue distribution, and apparent morphology (e.g., strong physiological-PS129 punctate labeling in grey matter). Considered together, PS129 has likely been underestimated due to postmortem intervals, and aSyn misfolding that preserves PS129 modification seems a probable explanation for pathological enrichment.

Potential pitfalls for these studies include the use of brain tissue from epileptic patients, which may have abnormally elevated PS129 due to neuronal hyperactivity and thus may not represent normal/basal PS129 levels. However, we didn't see evidence of gross hyperactivity (i.e., c-Fos) in the samples with high PS129, making it less likely that abnormal neuronal activity accounts for high PS129. Furthermore, the monkey brain had very high PS129, in the absence of c-Fos elevations or any known disease state. Temporal lobectomy tissues were optimal to test the hypothesis here because a known region of high PS129 in lower mammals, which could be rapidly preserved after resection, bears Lewy pathology in PD. Brain specimens for surgically resected tumors can vary by brain region and thus are less optimal for establishing physiological PS129. It is also worth noting that the procedure of surgical resection can itself potentially increase neuronal hyperexcitability due to mechanical tissue damage during resection.

Although critical, exact fixation times cannot be determined for each surgical case, due to the differences in length of surgical procedures, lag times between resection and placing tissue in fixative diffusion, as well as the unknown rate of fixative diffusion in the variably sized surgical samples. However, evidence here strongly suggests that delay to fixation is the critical parameter for measuring PS129 levels, as the highest ratios measured in the human brain were from a surgical case where specimens were immediately placed in fixative (TC1 and HIP1). Intriguingly, TC5 had the lowest PS129:asyn ratio and had the longest delay to fixation (10-15 min).

In conclusion, results showed a higher basal level of PS129 in the human brain than previously estimated. These measurements raise important questions about the hypothesized active role for PS129 in the pathological asyn aggregation process. Instead, recent findings make it likely that preservation of constitutive phosphorylation via alpha-synuclein misfolding could account for apparent pathological enrichment.

Acknowledgements

We would like to thank the tissue donors and brain banks for supplying valuable tissues. Thank you to the Rush Movement Disorders Brain Bank and Banner Sun Health Research Institute. Funding was provided by NINDS and NIA 5R01NS128467.

Figure Captions

Figure 1. PS129 in surgically resected brain is CIAP sensitive. IHC staining for PS129 in (A) hippocampus, (B) temporal lobe from surgical specimens, and (C) PD hemisections (Sample IDs in Table 1: HIP2, TC5, and PD HIP3, respectively). Sections were labeled using nickel-enhanced DAB chromogen (black) and counterstained with methyl green (green). Whole-section scans are shown with red and blue boxes denoting regions displayed in the high-magnification insets of select PS129-positive regions. A, B. PS129 immunoreactivity in surgical samples is apparent in specific regions within the sections, while CIAP and PK treatments abolish the signals in these samples. C. PS129 in PD hemisections demonstrates that aggregated PS129 is mostly detected in grey

matter throughout the hemisection, and CIAP pretreatment did not abolish PS129 reactivity. Scale bars: A,B = 1 mm and 25 µm; C = 1 cm and 3 µm. (n=3-5)

Figure 2. PS129 in surgical samples is sensitive to Proteinase K (PK) and CIAP. 10 µg of tissue lysate protein from each case was separated on 4–12% Bis–Tris gel, transferred onto PVDF membrane, and stained for total protein (Revert 700 Total Protein Stain, LI-COR), PS129, or αSyn. A Representative blot images showing total protein stain and chemiluminescence for PS129 and αSyn (BD SYN1) from surgical hippocampus, temporal cortex, and PD hippocampus samples (Specimen IDs in Table 1: HIP1, TC1, and PD HIP3, respectively). Negative controls (NC) indicate samples without enzymatic treatment. CIAP or PK represents tissues underwent pre-treatment of CIAP or PK. B,C PS129 and αSyn band intensities were first normalized to total protein (i.e., loading control) and then normalized to the mean intensity for each group. The left panel shows the normalized protein abundance for all samples compared to their negative controls (mean ± SD, Tukey's multiple comparisons test, *p-adj. < 0.05, **p-adj. < 0.01). The right panel shows paired individual values demonstrating abundance changes within the same samples under different enzymatic conditions. n=2-4.

Figure 3. PS129 to αSyn ratio in surgical and PD/DLB hippocampal tissues. Dot blot analysis was performed to evaluate the abundance of PS129 compared to total αSyn in surgical and PD/DLB hippocampal samples. 1 µl of each sample solubilized in crosslink reversal buffer was spotted onto methanol-activated PVDF membranes and subsequently probed for total protein, PS129 or αSyn. Sample IDs shown follow the

specimen IDs from Table 1. A Dot blots results from the surgical temporal cortex (TC) and hippocampus (HIP) are presented. Membranes were imaged simultaneously using optimal auto-exposure settings on a ChemiDoc imager (Bio-Rad). B Densitometry measurements were conducted concurrently using ImageJ software, and the resulting PS129:α-Syn ratios are displayed as a scatter plot. C PD/DLB hippocampal samples were processed identically to the surgical samples and immunoblotted for PS129 and or αSyn (EPR20535). D A scatter plot illustrating quantified PS129:αSyn ratios from PD/DLB dot blots.

Figure 4. PS129 to αSyn ratios in monkey and mouse samples. Coronal forebrain sections of the monkey brain, including the hippocampus, were immunostained for PS129 with and without CIAP. PS129 signals are mostly observed in grey matter, while CIAP treatment eliminated PS129 reactivity. Scale bars= 0.5 mm and 25 µm. Dot blot analysis was performed to evaluate the abundance of PS129 compared to total αSyn (BD SYN1) in monkey (B) and mouse (D) hippocampal tissues and cortical tissues adjacent to hippocampus. 1 µl of each sample solubilized in reversal buffer was spotted onto PVDF membranes and subsequently probed for total protein and PS129 or αSyn. Resulting dot blots for monkey (D) and mouse (E) were analyzed using ImageJ and PS129:α-Syn ratios are displayed as scatter plots. n=5

Figure 5. Physiological PS129 is not detected in post-mortem hippocampus with short post-mortem intervals (PMI=2-3h). IHC staining for PS129 in the hippocampus of control (non-synucleinopathy) and PD/DLB cases. Displayed cases are Short PMI control HIP 1

(top) and Short PMI PD HIP 1 (bottom) from Table 1. Tissues were treated with and without CIAP. Scale bars = 1 mm and 10 µm. n=3

References

1. Okochi, M., et al., *Constitutive phosphorylation of the Parkinson's disease associated alpha-synuclein.* J Biol Chem, 2000. **275**(1): p. 390-7.
2. Fujiwara, H., et al., *alpha-Synuclein is phosphorylated in synucleinopathy lesions.* Nat Cell Biol, 2002. **4**(2): p. 160-4.
3. Killinger, B.A., et al., *Distribution of phosphorylated alpha-synuclein in non-diseased brain implicates olfactory bulb mitral cells in synucleinopathy pathogenesis.* NPJ Parkinsons Dis, 2023. **9**(1): p. 43.
4. Ghanem, S.S., et al., *alpha-Synuclein phosphorylation at serine 129 occurs after initial protein deposition and inhibits seeded fibril formation and toxicity.* Proc Natl Acad Sci U S A, 2022. **119**(15): p. e2109617119.
5. McFarland, N.R., et al., *Alpha-synuclein S129 phosphorylation mutants do not alter nigrostriatal toxicity in a rat model of Parkinson disease.* J Neuropathol Exp Neurol, 2009. **68**(5): p. 515-24.
6. Azeredo da Silveira, S., et al., *Phosphorylation does not prompt, nor prevent, the formation of alpha-synuclein toxic species in a rat model of Parkinson's disease.* Hum Mol Genet, 2009. **18**(5): p. 872-87.
7. Karampetsou, M., et al., *Phosphorylated exogenous alpha-synuclein fibrils exacerbate pathology and induce neuronal dysfunction in mice.* Sci Rep, 2017. **7**(1): p. 16533.

8. Samuel, F., et al., *Effects of Serine 129 Phosphorylation on alpha-Synuclein Aggregation, Membrane Association, and Internalization.* J Biol Chem, 2016. **291**(9): p. 4374-85.
9. Ramalingam, N., C. Haass, and U. Dettmer, *Physiological roles of alpha-synuclein serine-129 phosphorylation - not an oxymoron.* Trends Neurosci, 2024. **47**(7): p. 480-490.
10. Ramalingam, N., et al., *Dynamic physiological alpha-synuclein S129 phosphorylation is driven by neuronal activity.* NPJ Parkinsons Dis, 2023. **9**(1): p. 4.
11. Parra-Rivas, L.A., et al., *Serine-129 phosphorylation of alpha-synuclein is an activity-dependent trigger for physiologic protein-protein interactions and synaptic function.* Neuron, 2023. **111**(24): p. 4006-4023 e10.
12. Muntane, G., I. Ferrer, and M. Martinez-Vicente, *alpha-synuclein phosphorylation and truncation are normal events in the adult human brain.* Neuroscience, 2012. **200**: p. 106-19.
13. Choi, S.G., et al., *Alpha-synuclein aggregates are phosphatase resistant.* Acta Neuropathol Commun, 2024. **12**(1): p. 84.
14. Walton, S., et al., *Neither alpha-synuclein fibril strain nor host murine genotype influences seeding efficacy.* NPJ Parkinsons Dis, 2024. **10**(1): p. 105.
15. Giasson, B.I., et al., *A hydrophobic stretch of 12 amino acid residues in the middle of alpha-synuclein is essential for filament assembly.* J Biol Chem, 2001. **276**(4): p. 2380-6.
16. Miake, H., et al., *Biochemical characterization of the core structure of alpha-synuclein filaments.* J Biol Chem, 2002. **277**(21): p. 19213-9.
17. Spillantini, M.G., et al., *alpha-Synuclein in filamentous inclusions of Lewy bodies from Parkinson's disease and dementia with lewy bodies.* Proc Natl Acad Sci U S A, 1998. **95**(11): p. 6469-73.
18. Tanji, K., et al., *Proteinase K-resistant alpha-synuclein is deposited in presynapses in human Lewy body disease and A53T alpha-synuclein transgenic mice.* Acta Neuropathol, 2010. **120**(2): p. 145-54.
19. Selikhova, M., et al., *A clinico-pathological study of subtypes in Parkinson's disease.* Brain, 2009. **132**(Pt 11): p. 2947-57.
20. Foltynie, T., C. Brayne, and R.A. Barker, *The heterogeneity of idiopathic Parkinson's disease.* J Neurol, 2002. **249**(2): p. 138-45.
21. Takeda, A., et al., *C-terminal alpha-synuclein immunoreactivity in structures other than Lewy bodies in neurodegenerative disorders.* Acta Neuropathol, 2000. **99**(3): p. 296-304.
22. Volpicelli-Daley, L.A., K.C. Luk, and V.M. Lee, *Addition of exogenous alpha-synuclein preformed fibrils to primary neuronal cultures to seed recruitment of endogenous alpha-synuclein to Lewy body and Lewy neurite-like aggregates.* Nat Protoc, 2014. **9**(9): p. 2135-46.
23. Schlabitz, S., et al., *Spatiotemporal Correlation of Epileptiform Activity and Gene Expression in vitro.* Front Mol Neurosci, 2021. **14**: p. 643763.
24. Morgan, J.I., et al., *Mapping patterns of c-fos expression in the central nervous system after seizure.* Science, 1987. **237**(4811): p. 192-7.
25. Willoughby, J.O., et al., *Distribution of Fos-positive neurons in cortical and subcortical structures after picrotoxin-induced convulsions varies with seizure type.* Brain Res, 1995. **683**(1): p. 73-87.
26. Barros, V.N., et al., *The pattern of c-Fos expression and its refractory period in the brain of rats and monkeys.* Front Cell Neurosci, 2015. **9**: p. 72.
27. Bakker, R., P. Tiesinga, and R. Kötter, *The Scalable Brain Atlas: Instant Web-Based Access to Public Brain Atlases and Related Content.* Neuroinformatics, 2015. **13**(3): p. 353-366.

28. Lin, X., et al., *c-Fos mapping of brain regions activated by multi-modal and electric foot shock stress.* Neurobiol Stress, 2018. **8**: p. 92-102.
29. Pompeiano, M. and M.T. Colonnese, *cFOS as a biomarker of activity maturation in the hippocampal formation.* Front Neurosci, 2023. **17**: p. 929461.
30. Dienel, G.A., *Stop the rot. Enzyme inactivation at brain harvest prevents artifacts.* Journal of Neurochemistry, 2021. **158**(5): p. 1007-1031.
31. Wang, Y., et al., *Rapid alteration of protein phosphorylation during postmortem: implication in the study of protein phosphorylation.* Scientific Reports, 2015. **5**(1): p. 15709.

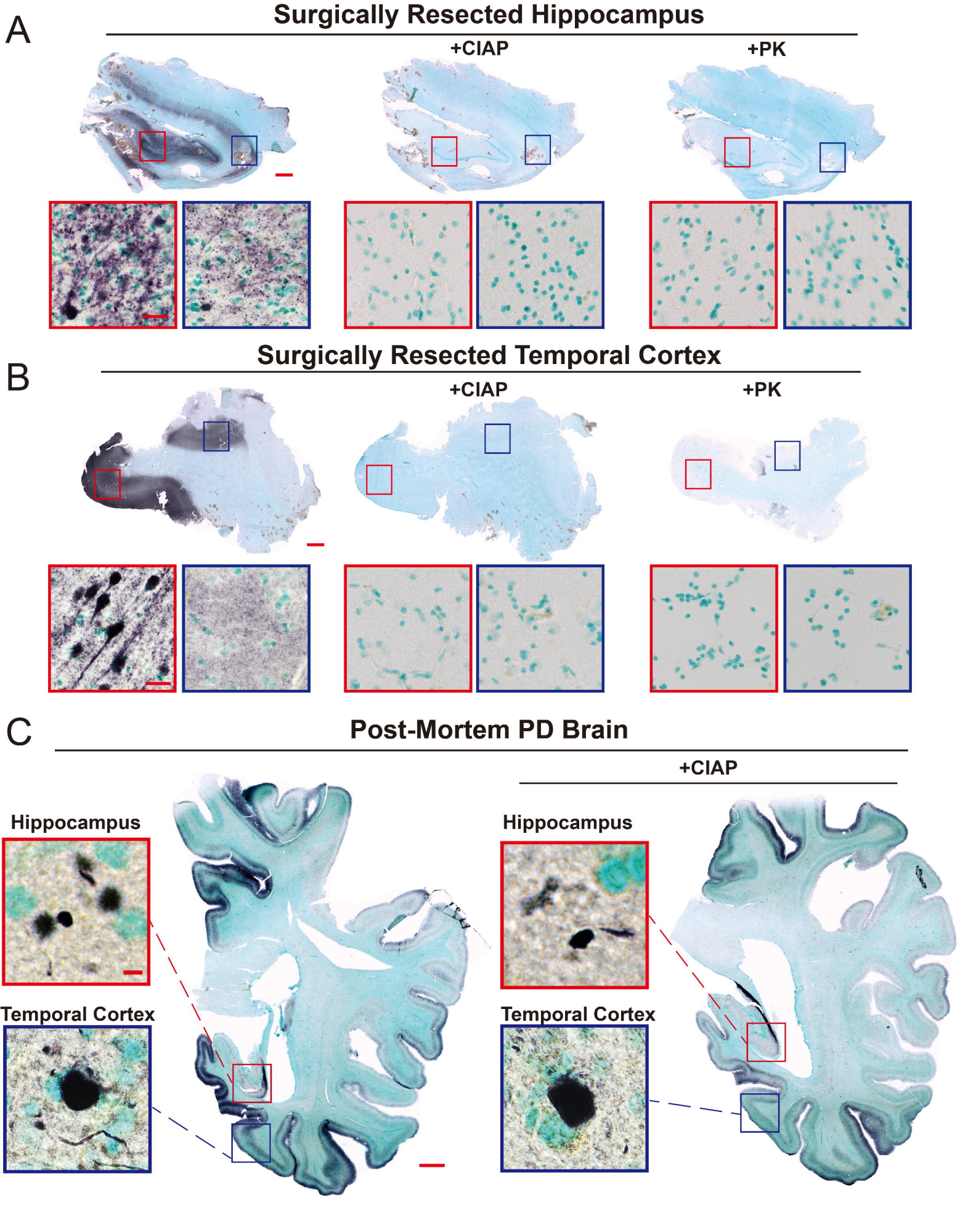
A
Surgically Resected Hippocampus
+CIAP
+PK
B
Surgically Resected Temporal Cortex
+CIAP
+PK
C
Post-Mortem PD Brain
+CIAP
Hippocampus
Temporal Cortex
Hippocampus
Temporal Cortex

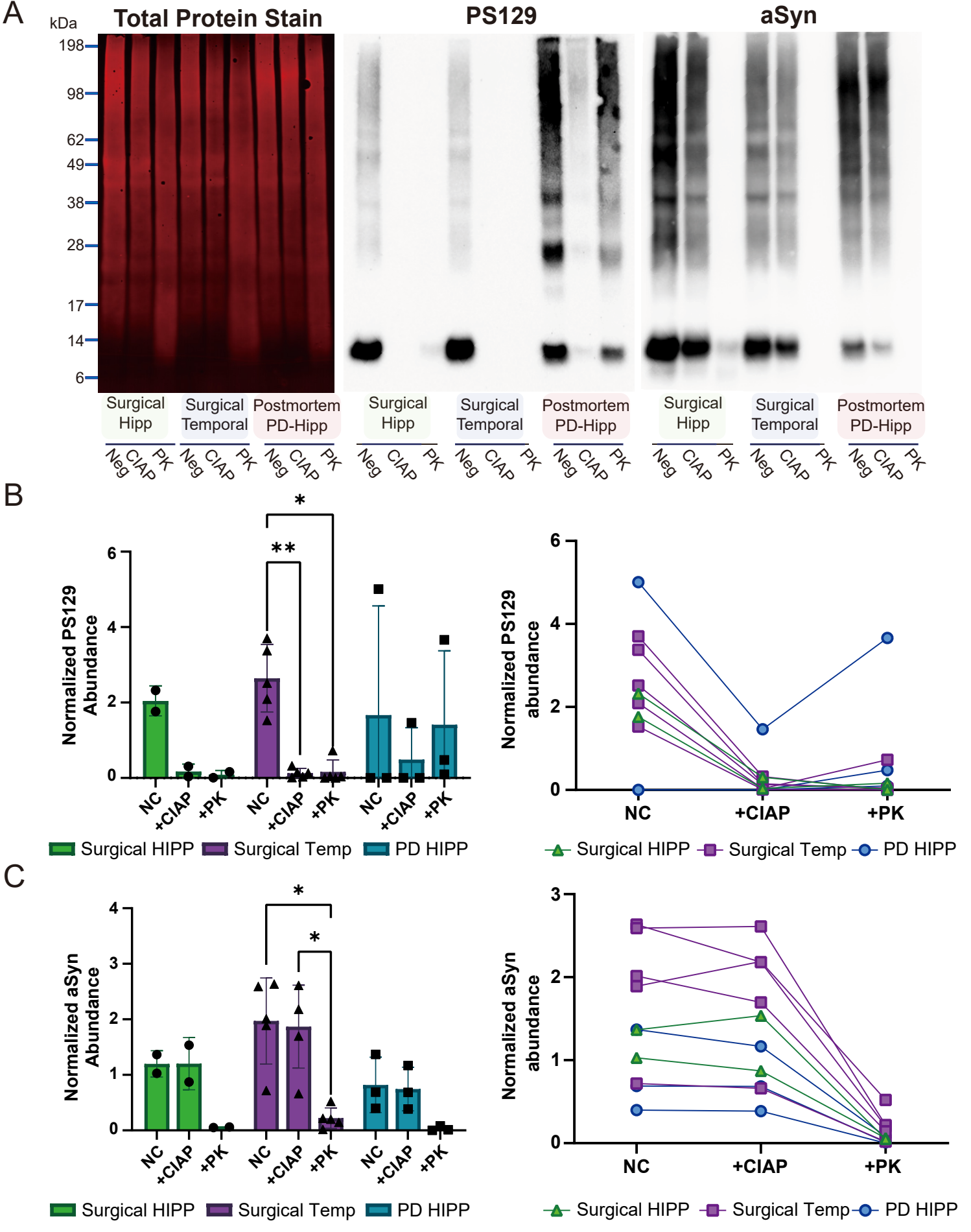
A
kDa
Total Protein Stain
PS129
aSyn
198
98
62
49
38
28
17
14
6
Surgical Hipp
Surgical Temporal
Postmortem PD-Hipp
Neg
CIAP
PK
B
Normalized PS129 Abundance
NC
+CIAP
+PK
Surgical HIPP
Surgical Temp
PD HIPP
Normalized PS129 abundance
C
Normalized aSyn Abundance
Normalized aSyn abundance

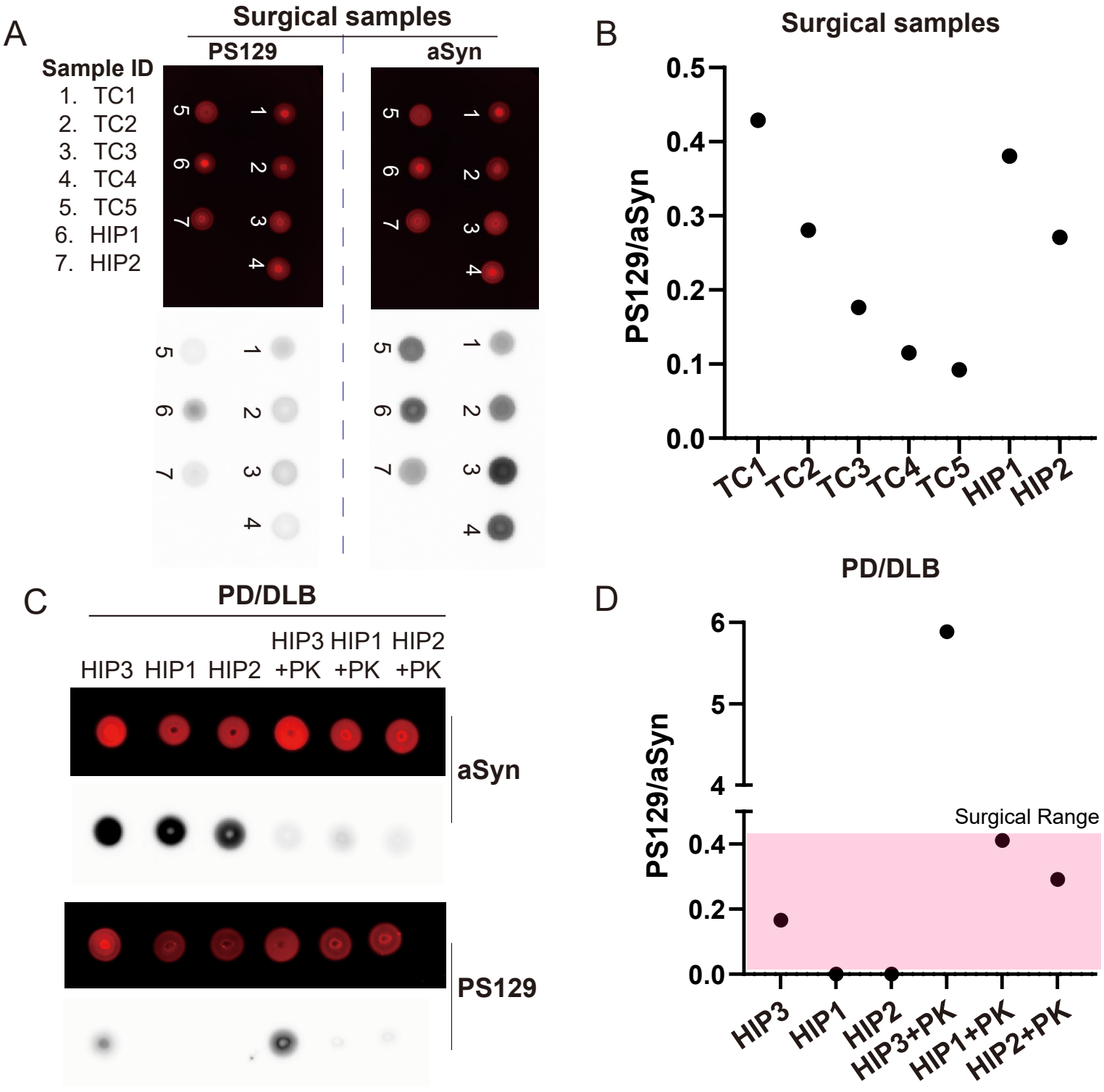
A
Surgical samples
PS129
aSyn
Sample ID
1. TC1
2. TC2
3. TC3
4. TC4
5. TC5
6. HIP1
7. HIP2
B
Surgical samples
PS129/aSyn
0.5
0.4
0.3
0.2
0.1
0.0
TC1
TC2
TC3
TC4
TC5
HIP1
HIP2
C
PD/DLB
HIP3
HIP1
HIP2
HIP3 +PK
HIP1 +PK
HIP2 +PK
aSyn
PS129
D
PD/DLB
PS129/aSyn
6
5
4
0.4
0.2
0.0
Surgical Range
HIP3
HIP1
HIP2
HIP3+PK
HIP1+PK
HIP2+PK

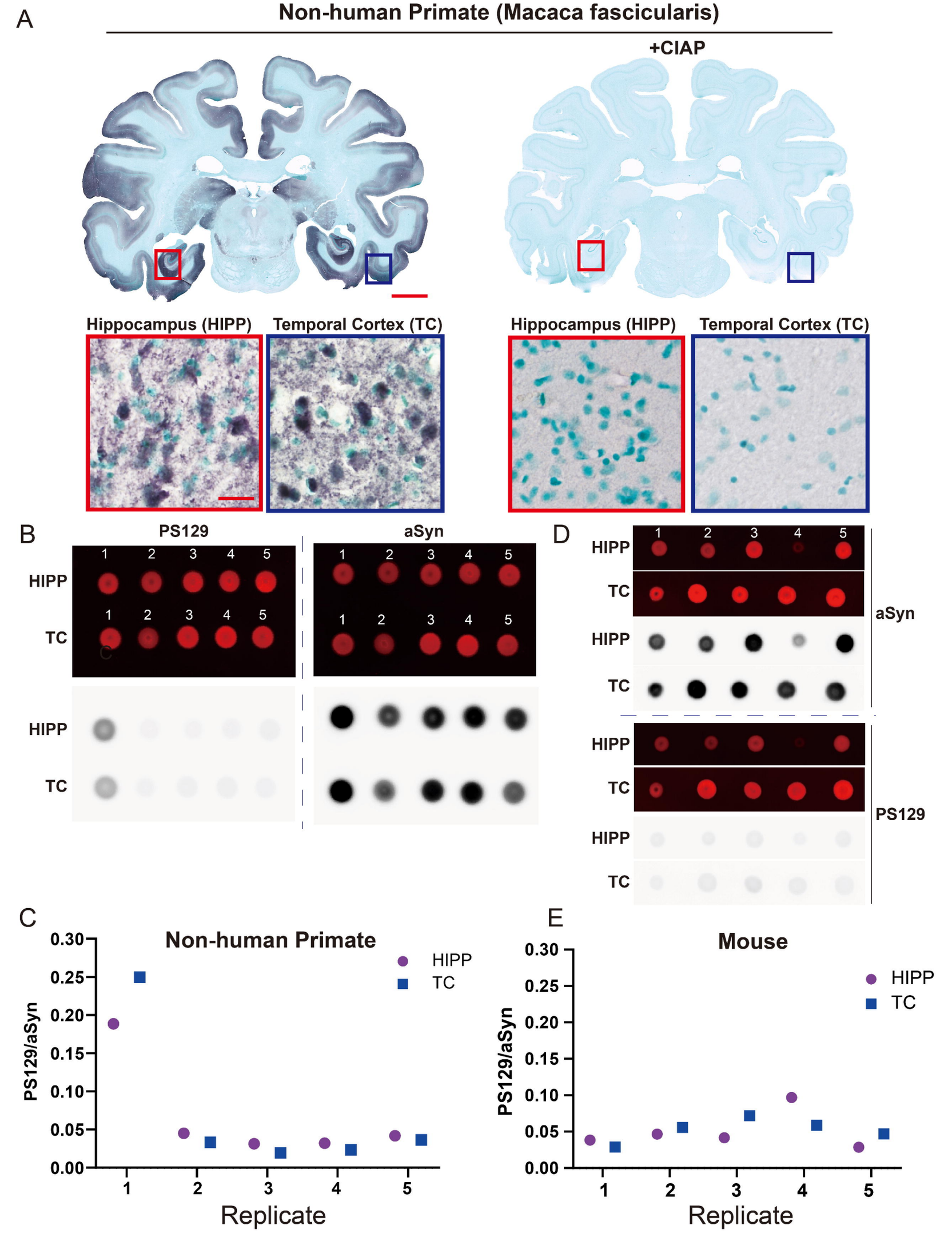
A
Non-human Primate (Macaca fascicularis)
+CIAP
Hippocampus (HIPP)
Temporal Cortex (TC)
Hippocampus (HIPP)
Temporal Cortex (TC)
B
PS129
aSyn
HIPP
TC
HIPP
TC
D
HIPP
TC
aSyn
HIPP
TC
HIPP
TC
PS129
HIPP
TC
C
Non-human Primate
HIPP
TC
PS129/aSyn
Replicate
E
Mouse
HIPP
TC
PS129/aSyn
Replicate

Non-synucleinopathy Hippocampus

+CIAP

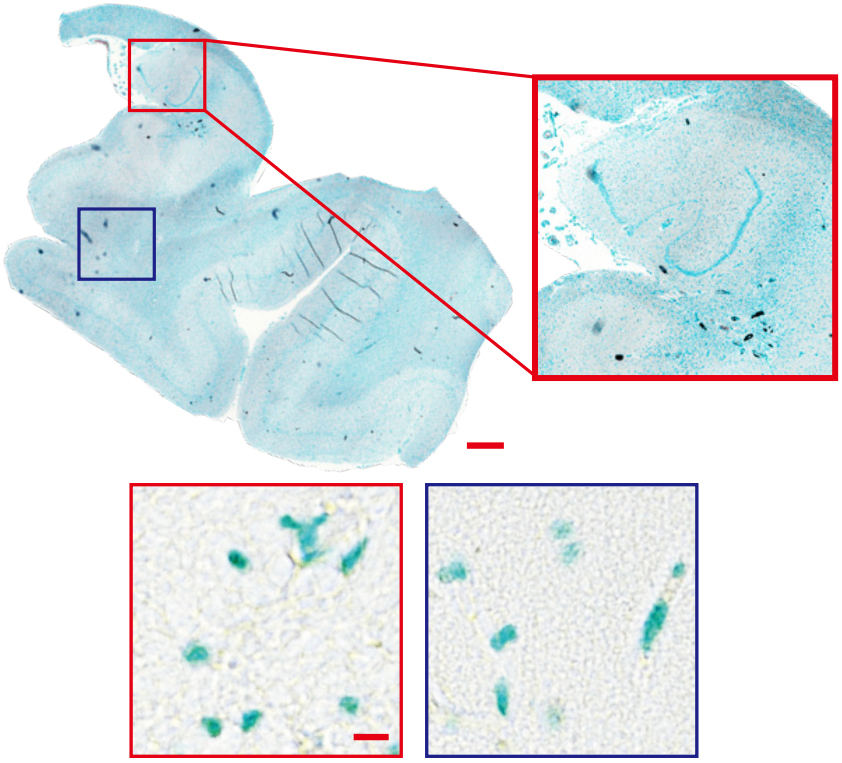

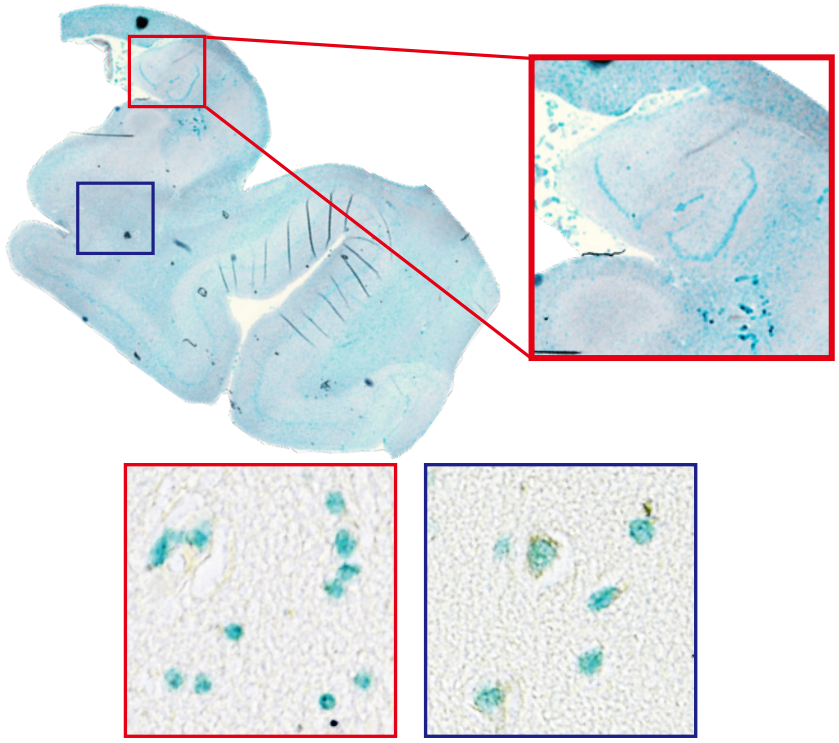

PD Hippocampus
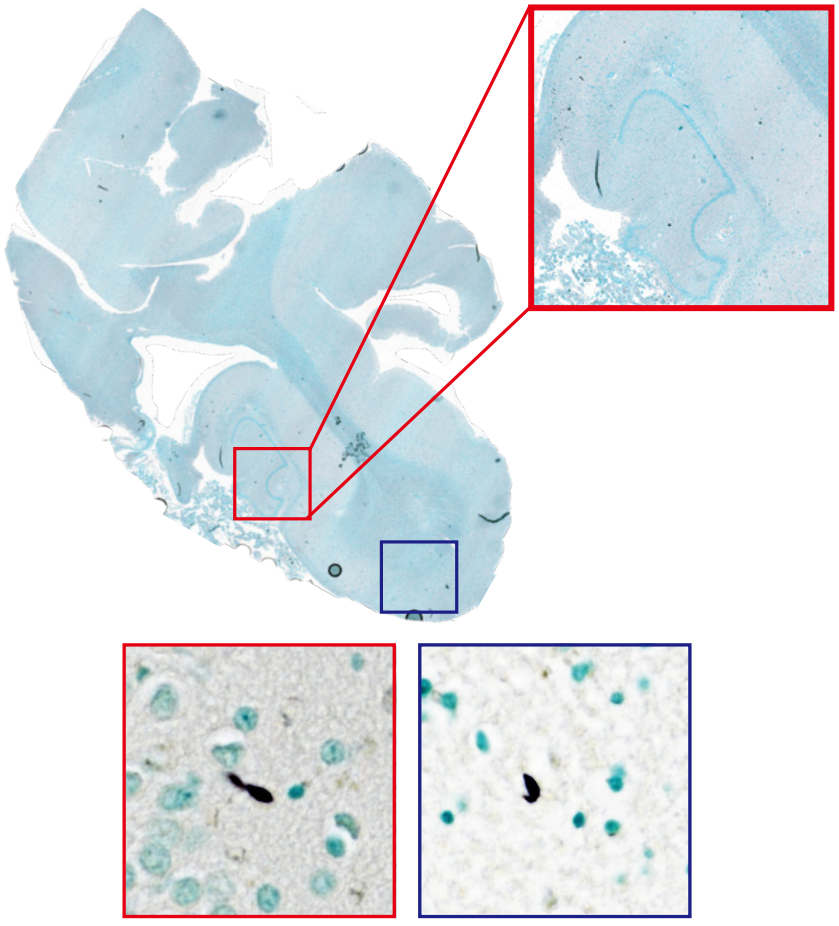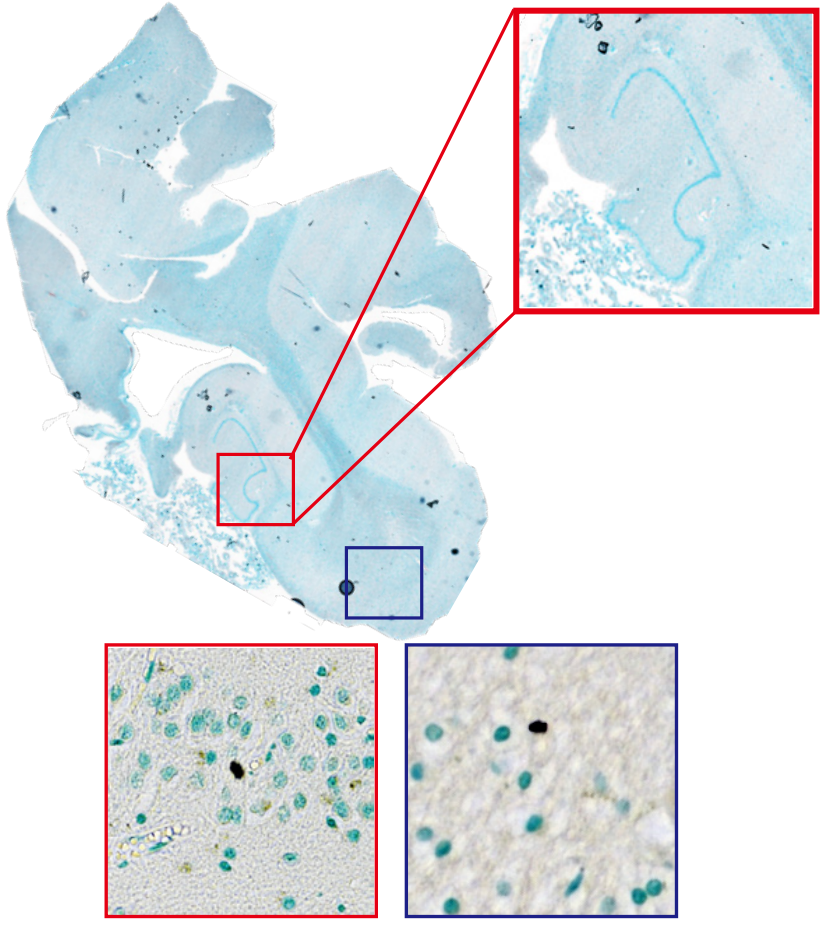
+CIAP